

# Phase Transitions and Structure of Polymer Systems in External Fields



# Phase Transitions and Structure of Polymer Systems in External Fields

By

Sergey A. Vshivkov

Cambridge  
Scholars  
Publishing



Phase Transitions and Structure of Polymer Systems in External Fields

By Sergey A. Vshivkov

*Reviewers:*

*A.Y. Zubarev*, Prof. Dr. of Physical & Mathematical Sciences (Ural Federal University)

*V.G. Buryndin*, Prof. Dr. of Technical Sciences (Urals State Forestry Engineering University)

This book first published 2019

Cambridge Scholars Publishing

Lady Stephenson Library, Newcastle upon Tyne, NE6 2PA, UK

British Library Cataloguing in Publication Data

A catalogue record for this book is available from the British Library

Copyright © 2019 by Sergey A. Vshivkov

All rights for this book reserved. No part of this book may be reproduced, stored in a retrieval system, or transmitted, in any form or by any means, electronic, mechanical, photocopying, recording or otherwise, without the prior permission of the copyright owner.

ISBN (10): 1-5275-3296-8

ISBN (13): 978-1-5275-3296-0

# CONTENTS

Abstract .....	x
Preface .....	xi
Introduction .....	1
<b>Part I. Phase Transitions in Polymer Systems accompanied by Amorphous and Crystalline Phase Separation</b>	
Chapter 1 .....	4
General Overview of Phase Equilibrium	
1.1 Types of Diagrams of Polymer–Solvent Systems .....	8
1.2 Impact of Size and Shape of Solvent Molecules on Phase Transitions .....	17
1.3 Classification of Phase Transitions .....	23
Chapter 2 .....	26
Phase Transitions in Polymer Solutions induced by Mechanical Field	
2.1 Dynamic Structure Formation in Polymer Solutions .....	26
2.2 Phase Transitions in Melts and Solutions of Crystalline Polymers Induced by Mechanical Field .....	31
2.3 Influence of Deformation on Phase Transitions in Amorphous Polymer Solutions .....	38
2.4 Phase Transitions in Deformed Gel-forming Systems .....	49
Chapter 3 .....	51
Compatibility between the Components of Rubber-Containing Blends and Solutions under Static Conditions and in Mechanical Field	
3.1 Phase Diagrams of Rubber Blends under Static Conditions .....	52
3.2 Phase Transitions in Deformed Rubber Blends .....	58
3.3 Phase Transitions in Polymer-Polymer-Solvent Systems .....	59

Chapter 4 .....	70
Theoretical Justification of Phase Transitions in Polymer Solutions induced by Mechanical Field	
4.1 Liquid-Liquid Phase Separation.....	70
4.2 Crystalline Phase Separation.....	75
Chapter 5 .....	82
Phase Transitions in Polymer Blends induced by Mechanical Field	
5.1 Experimental Data .....	82
5.2 Theoretical Concepts .....	97
Chapter 6 .....	108
Phase Transitions in Nonelectrolyte Cross-linked Polymer Gels under Deformation	
6.1 Phase Diagrams.....	110
6.2 Pulsing Mechanism of Phase Separation of Gels.....	114
6.3 Deformation Impact on Thermodynamic Stability and Phase Transitions of Polymer Gels.....	119
Chapter 7 .....	128
Impact of External Pressure on Phase Behavior of Polymer Systems	
7.1 Pressure Effects on Solubility of Amorphous Substances .....	128
7.2 Pressure Effect on Solubility of Crystalline Substances .....	129
7.3 Pressure Effect on Critical Solution Temperatures .....	130
7.4 Negative Pressure Effect on Phase Transitions in Polymer Solutions.....	135
Chapter 8 .....	137
Phase and Structural Transitions of Polymer Systems in Electric Field	
Chapter 9 .....	140
Methods of Calculation of Boundary Curves, Critical and $\Theta$ -Temperatures: Comparison with Experimental Results	
9.1 Calculations Based on Flory-Huggins Theory .....	140
9.2 Calculations Based on Prigogine–Patterson Theory and Flory Theory .....	144
9.3 Effects of Precipitators on Phase Equilibrium of Polystyrene Solutions Close to Upper and Lower Critical Solution Temperatures.....	159
9.4 Phase Diagrams and Thermodynamic Interaction Parameter of Components of Deformed Polymer Systems .....	168

**Part II. Liquid Crystalline Phase Transitions in Polymer Systems**

Chapter 1 .....	178
Liquid Crystalline State of Matter	
1.1 Specific behavior of polymer liquid crystalline (LC) state .....	187
Chapter 2 .....	190
Phase Diagrams of Solutions of Rigid-Chain Polymers	
2.1 Effect of Molecular Weight of Polymer on Liquid Crystalline Phase Transitions in Cellulose Ester–Solvent Systems .....	199
2.2 Effect of Polymer Chemical Structure on Liquid Crystalline Phase Transitions .....	201
2.3 Effect of Solvent Nature on Liquid Crystalline Phase Transitions .....	205
2.4 Phase Transitions in Water Solutions of Hydroxypropyl Cellulose .....	209
Chapter 3 .....	212
Self-Assembly of Nanodimensional Molecules of Cellulose Esters	
3.1 Self-assembly of Macromolecules in Solutions of Rigid-Chain Polymers .....	212
3.2 Effect of Magnetic Field on Size of Supramolecular Particles in Solutions of Cellulose Derivatives .....	222
3.3 Calculation of Number of Molecules in Supramolecular Particles .....	225
Chapter 4 .....	233
Phase Transitions and Structure of Liquid Crystalline Systems in Mechanical Field	
4.1 Phase Transitions and Structure in Deformed Liquid Crystalline Systems .....	233
4.2 Enthalpy of Activation of Viscous Flow .....	242
Chapter 5 .....	247
Phase Transitions and Structure of Liquid Crystalline Systems in Magnetic Field	
5.1 Effect of Magnetic Field on Liquid Crystalline Systems .....	247
5.2 Phase Transitions and Structure of Solutions of Cellulose Esters in Magnetic Field .....	250
5.3 Effect of Intensity of Magnetic Field on Phase Transitions .....	258
5.4 Effect of Polymer Concentration on Phase Transitions .....	261

5.5. Magnetic Field Energy Stored by Solutions and Temperature of Phase Transitions .....	265
----------------------------------------------------------------------------------------------	-----

### **Part III. Experimental Methods of Phase Diagrams Building, Determination of Critical Temperatures and $\Theta$ -Temperatures**

Chapter 1 .....	271
Methods Based on Measurements of Optical Characteristics	
1.1 Cloud Point Method.....	271
1.2 Light Scattering at Big Angles.....	275
1.3 Critical Opalescence Method.....	278
1.4 Pulse-induced Light Scattering.....	279
1.5 Measurement of Optical Density and Turbidity.....	280
1.6 Method of Turbidimetric Titration.....	280
1.7 Refractometric Method.....	281
1.8 Interferential Micromethod.....	282
1.9 Method of Polarization Microscopy.....	283
Chapter 2 .....	285
Spectroscopic Technique	
2.1 IR Spectroscopy.....	285
2.2 Nuclear Magnetic Resonance.....	286
2.3 Paramagnetic Probe Method.....	287
2.4 Spin Label Method.....	288
2.5 Dielectric Method .....	288
Chapter 3 .....	290
Thermophysical Methods	
3.1 Dilatometry .....	290
3.2 Differential Thermal Analysis, Differential Scanning Calorimetry .....	290
Chapter 4 .....	291
Methods Fixing Transfer of Component Mass	
4.1 Viscometric Methods.....	291
4.2 Diffusion Method.....	293
4.3 Reversed-Phase Gas Chromatography Method.....	293
4.4 Centrifugation Method.....	294
4.5 Determination of Compositions and Volume Ratio of Coexisting Phases .....	294



Chapter 5 .....	296
Thermodynamic Methods	
5.1 Determination of Second Virial Coefficients.....	296
5.2. Method of Restricted Swelling .....	296
5.3 Determination of Interphase Energy .....	297
5.4 Determination of Vapor Pressure.....	297
5.5 Determination of Solubility Parameters.....	298
5.6 Dynamic Osmometry Method.....	298
Chapter 6 .....	299
Temperature Diffractometry and Scattering of Neutrons	
6.1 Temperature Diffractometry .....	299
6.2 Neutron Scattering .....	299
Chapter 7 .....	300
Results of Phase Equilibrium Investigation obtained by using Different Methods in Polymer Solutions	
Conclusion.....	310
References .....	315
Abbreviations and Symbols.....	361

## ABSTRACT

The present monograph summarizes and analyzes the results of studies on phase transitions in polymer solutions, blends and gels induced by the mechanical field (tension stress, compression, shear deformation, positive and negative external pressure), electric and magnetic fields and beyond fields over the last 60 years. The systems with amorphous (liquid) separation with upper and lower critical solution temperatures, crystalline phase separation and liquid-crystalline transitions are considered.

The effects of molecular weight, chain flexibility, polymer concentration, polarity and sizes of solvent molecules, deformation rate, magnetic field intensity, and interfacial energy on phase transitions in polymer systems under mechanical, magnetic and electric fields are analyzed. Phase diagrams and the pulsating mechanism of phase separation of the gels of cross-linked polymers are described. The methods of plotting and calculation of phase diagrams in polymer systems are discussed.

The monograph "Phase Transitions and Structure of Polymer Systems in External Fields" will be useful for scientific researchers, postgraduate students and students specializing in the phase transitions in multicomponent systems.

## PREFACE

The monograph presents summarized and analyzed data on phase amorphous, crystalline, liquid crystal transitions in polymer systems in magnetic, mechanical, electric fields and beyond fields.

The first part of the book describes various types of phase diagrams, processes of dynamic structure formation, and preceding amorphous and crystalline phase transitions in shearing and longitudinal fields. The authors discuss the effects of molecular weight, polymer concentration, relationship of the surface energy components, sizes and shapes of solvent molecules, electric field, shear rate, and external pressure on the position of the boundary curves in polymer solutions, blends and gels. The monograph presents the theoretical assumptions on the influence of external fields on the thermodynamic stability of the polymer systems. The methods of calculating boundary curves, critical temperatures and  $\theta$ -temperatures are described.

The second part deals with liquid-crystalline phase transitions. The influence of molecular weight, chemical structure and polymer concentration, polarity of solvent molecules, magnetic field intensity and shear deformation on the position of boundary curves of polymer-solvent systems separating isotropic regions from anisotropic regions are discussed. The self-organization of rigid macromolecules and the rheological properties of the system are described.

The third part contains information on the experimental methods used in the study of phase transitions. Almost all known methods of plotting phase diagrams of polymer systems and experimental procedures are described. This contributes to the creation of a unified approach and the requirements of the methods of diagram plotting and the interpretation of the results. The absence of such an approach causes the accumulation of contradictory information on the mutual solubility of the components in polymer systems.

The monograph is intended to be used by physical chemists and researchers of the synthesis and processing of polymers; it will also be useful for students and postgraduate students specializing in the physical chemistry of polymers.

The author acknowledges the great contribution by the official reviewers Prof. Dr. of Physical & Mathematical Sciences A.Y. Zubarev

and Prof. Dr. of Technical Sciences V.G. Buryndin for their close examination of the manuscript and valuable remarks.

The author thanks Prof., Dr. of Chemical Sciences Rusinova E.V. for the help in the preparation of this book.

## INTRODUCTION

The study of phase equilibrium in polymer systems is a crucial task since phase transitions determine the structure and the properties of the systems. The processes causing the appearance of new phases play a major role in polymerization and polycondensation, microencapsulation, adsorption from solutions, and production of fibers, membranes and films. Phase equilibrium studies are essential for the development of the theory of solutions since they provide an opportunity to verify theoretical assumptions, which is why it is quite natural that a lot of attention is given to the issue of phase equilibrium [1-31]. Phase diagrams give complete information on the mutual solubility of components. This is the essence of their value.

In the USSR the first studies of phase equilibrium in polymer solutions were made by V.A. Kargin, S.P. Papkov and Z.A. Rogovin (*Zhurnal prikladnoy khimii*, 1937, V.10, No.1, pp. 156-157; No. 4-5, pp. 607-619). Significant contributions to the development of the views on thermal dynamics of polymer systems were made by P. Flory, R. Koningsfeld, G. Rehage, D. Patterson, A.A. Tager, S.Ya. Frenkel, A.E. Chalykh, V.P. Budtov, Yu.S. Lipatov, V.N. Kuleznev, V.I. Klenin, and others.

During operation and processing, polymer systems are exposed to different mechanical impacts. The polymer orientation enhancing their mechanical properties is mainly achieved through the directional mechanical effect. Molecular orientation caused by the deformation of melts or solutions and fixed by phase transition (crystallization) has opened up potentialities for producing high modulus fibers.

According to S.Ya. Frenkel, the mechanical impact results in the displacement of boundary curves: the binodal and liquidus curves. The theory of phase transitions in polymer systems perturbed by the mechanical field is far from complete (the mechanical field is a vector field of forces occurring in the system under deformation). In the last 60 years, many studies on the mechanical impact on phase transitions in polymer systems with amorphous and crystalline phase separation have been published. The majority of these works were reviewed by S.A. Vshivkov and E.V. Rusinova in *Phase Transitions in Polymer Systems Induced by Mechanical Field*. There is no doubt that mechanical stress can

be an independent thermodynamic factor determining the position of the binodal and liquidus curves.

Liquid-crystal systems play a special role in the studies. More than one hundred years ago, it was found that some organic substances, when being melted, i.e. having the capacity of flowing, exhibit anisotropic optical properties (birefringence). This circumstance formed the grounds for naming such substances liquid crystal (LC).

Given the fact that this phase appeared to be an intermediate state between the crystalline and amorphous states, it was called mesomorphic (“mesos” in Greece means “intermediary”, “in-between”). The practical application of liquid crystals began in the early 60<sup>th</sup>. When the liquid crystals were used in displays (watches, mini TV sets, etc.), LC displays for computers and other spheres, this caused a revolution in electronics. In 1991 P-G. de Gennes was awarded the Nobel Prize for his discovery that “the methods, developed for the study of ordering phenomenon in simple systems, can be generalized and used for the liquid crystal and polymers.”

The first scientist to state that the polymers are capable of forming mesophases was academician V.A. Kargin, who, in 1941, wrote that the “interaction between large molecules will be great enough even if the interaction of separate chains is rather weak. And the consequence ...can be the orientation of such large molecules in some general direction.” The theoretical analysis of such systems was carried out in 1950 by Professor Flory, the Nobel laureate, who proposed the phase diagram pattern for the above systems.

Phase transitions are always preceded by the self-organization of macromolecules. This process, enhanced by the application of external (magnetic, mechanical, electric) fields onto the polymer systems, can bring about both the displacement of boundary curves (binodal and liquidus curves) and changes in their shape related to the change of the phase transition type. The present monograph summarizes and analyzes the data on amorphous, crystalline and liquid crystalline phase transitions in polymer systems.

**PART I.**

**PHASE TRANSITIONS IN POLYMER SYSTEMS  
ACCOMPANIED BY AMORPHOUS  
AND CRYSTALLINE PHASE SEPARATION**

# CHAPTER 1

## GENERAL OVERVIEW OF PHASE EQUILIBRIUM

The modern development of the phase equilibrium theory is generally based on the classical works of Gibbs [1], Andrews [2] and Van der Waals [3]. A great contribution to these ideas, especially for liquid-liquid binary systems, was also made by Alekseev [4] and Konovalov [5]. Nowadays there is a great number of works describing the phase separation of low-molecular-weight liquid blends. Thus, in his monograph [6], Francis reports the data for nine hundred systems with liquid and crystalline phase separation. These two types of phase separation differ not only in the nature of formed phases (in the first case, both coexisting phases are liquids and in the second case, one of them is crystalline), but also in their phase diagrams, which are fundamentally different.

In the case of liquid-liquid phase separation, the boundary curves, which separate single-phase and two-phase regions, are represented by parabolas, the branches of which never cross the axes of ordinates with the temperature decrease but run parallel to them (Fig. 1.1, a). Any horizontal line crossing this curve connects the points, the abscissas of which correspond to the compositions of the coexisting phases. These lines are called *nodes*, and the curve is known as the *binodal*. When the temperature rises, the phase compositions converge, the nodes get shorter and finally degenerate to a point called the upper critical solution temperature (UCST). Often these temperatures are called the critical mixing temperatures. However, this is a less precise notion since not every mix leads to a dissolution. The binodal curve may be convex downward (see Fig. 1.1, b). In this case, a single-phase (homogenous) system separates upon heating and the lower critical solution temperature (LCST) is observed. The systems which have both critical solution temperatures (CSTs) are known (Fig. 1.1, c, d).

The phase diagram of a ternary system at constant temperature is represented by an equilateral triangle, the vertices of which correspond to 100% content of A, B and C components (see Fig. 1.1, d). Points a, b and c on the sides of the triangle correspond to the composition of the binary blends  $A - B$ ,  $B - C$  and  $A - C$ . The system composition is represented by



point O. Segments Oa, Ob and Oc, which are parallel to the triangle sides, correspond to the fractions of components A, B and C after demixing. A set of such points at phase separation temperature ( $T_{ph}$ ) represents a binodal.

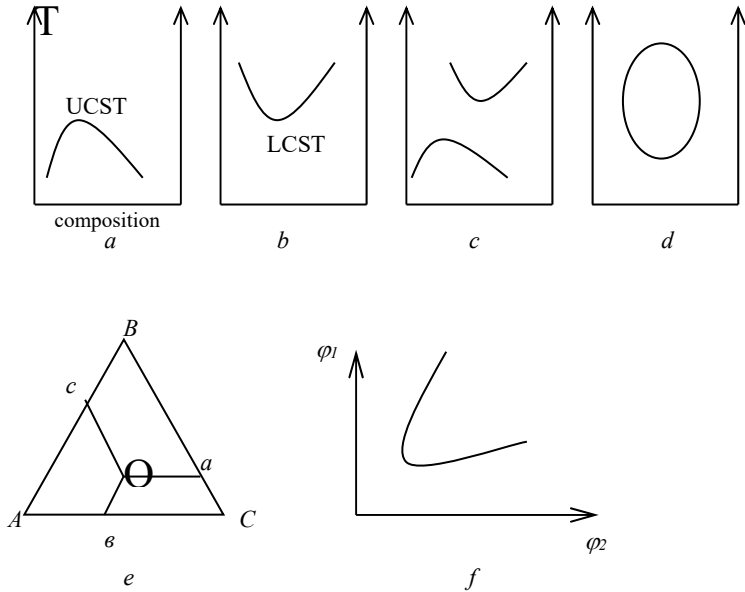


**Fig. 1.1.** Phase diagrams of liquid-liquid phase separation (see explanations in the text)

Another way to illustrate the phase equilibrium of ternary systems is to plot the dependence of the concentration of component 1 ( $\varphi_1$ ) versus the concentration of component 2 ( $\varphi_2$ ) in the coexistent phases. At the critical point, the component concentrations will be the same (Fig. 1.1, e).

In the case of liquid-solid phase separation, the boundary curve has another form (Fig. 1.2). This is the set of points corresponding to the temperatures and concentrations at which one of the components begins to crystallize out of the solutions. Such curves are called the *liquidus lines (curves)* and they are fundamentally different from the binodals in two aspects: the liquidus curves intersect the vertical axis at the points corresponding to the melting temperatures of the pure components while the horizontal lines (nodes) connect the points corresponding to the

coexistent phases; however, in this case, the temperature rise changes the composition of only one phase.

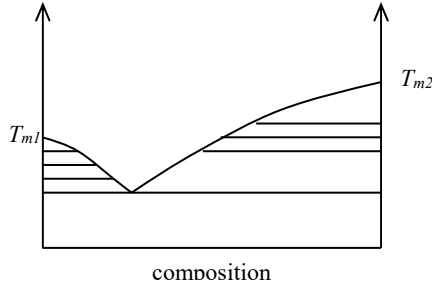


**Fig.1.2.** Phase diagram of metal 1 – metal 2 system ( $T_m$  is the melting temperature)

The study of critical phenomena shows a certain peculiarity, the uniqueness of the critical point, and its difference from all other binodal points, which are called phase separation temperatures. At the critical point, the interphase energy is equal to zero, which was first mentioned by Mendeleev. At the critical point, the maximum asymmetry of Rayleigh scattering (critical opalescence) [7], the abnormal values of dielectric properties [8, 9], viscosity [10, 11] as well as other properties [12–15] have been observed for the solutions.

The critical point of the liquid-liquid systems is characterized by the following thermodynamic equations:

$$\begin{aligned} [\partial\mu_i/\partial x_i]_{P,T} &= [\partial^2\mu_i/\partial x_i^2]_{P,T} = 0, \\ [\partial^3\mu_i/\partial x_i^3]_{P,T} &> 0, \end{aligned}$$

i.e. the first and the second derivatives of the chemical potential ( $\mu_i$ ) of each component ( $x_i$ ) are equal to zero while the third derivative is positive. This means that the  $\mu_i=f(x_i)$  dependence curve is bent at the critical point.

According to Prigogine and Defay [15],

for the UCST:

$$(\partial^2 h/\partial x_2^2)_{T_c} < 0 \text{ and } (\partial^2 s/\partial x_2^2)_{T_c} < 0 \quad (1.1), \text{ and}$$

for the LCST:

$$(\partial^2 h/\partial x_2^2)_{T_c} > 0 \text{ and } (\partial^2 s/\partial x_2^2)_{T_c} > 0,$$

where  $h$  and  $s$  are the average enthalpy and entropy of the mixing.

It follows from equation (1.1) that [15]:

for the UCST:

$$h^E > 0, s^E > 0, \text{ and}$$

for the LCST (1.2):

$$h^E < 0, s^E < 0,$$

where  $h^E$  and  $s^E$  are the excess enthalpy and entropy of the system formation, which characterize deviations of these parameters from the ideal values.

Equations (1.1) and (1.2) are the thermodynamic criteria for the existence of UCST and LCST. The systems with UCST are characterized by the endothermic mixing and the entropy of mixing, which exceed the ideal value. The systems with LCST are characterized by the exothermic mixing and the entropy of mixing, which are less than the ideal value.

Some authors doubted the uniqueness of the critical point, assuming the existence of a critical region instead of a single critical point. Such assumptions were made by Avenarius [16]. He later retracted it. Subsequently, Mayer [17 – 19] developed a theory of critical regions, which was strongly criticized by many famous experts in thermodynamics. Krichevsky and Rosen [20], Geilikman [21] and Dubrovsky [22] revealed some mathematical errors and arbitrary assumptions in Mayer's theory. Golik et al. [23, 24] showed fallacies in the experimental results obtained by Maas [25], which served as the basis for the critical region theory. Therefore, the existence of a critical region is completely denied at present. The binodal equation represents the equality of the chemical potentials of the components in the coexistent phases:

$$\mu_i (\text{I}) = \mu_i (\text{II}), \Delta\mu_i (\text{I}) = \Delta\mu_i (\text{II})$$

Within the binodal curve there is a region bound by the spinodal curve. The spinodal equation has the following view:

$$[\partial^2 \Delta G / \partial x_i^2]_{p, T} = 0, [\partial^2 \Delta G / \partial \omega_i^2]_{p, T} = 0,$$

where  $x_i$  is the mole fraction ( $\omega_i$  is the mass fraction) of the  $i^{\text{th}}$  component.

The spinodal curve has one common point with the binodal curve. This point is called the critical point. The binodal separates the region of stable solutions from the metastable region while the spinodal curve separates the region of metastable solutions from the unstable (labile) region and determines the boundary of the system's absolute instability. Its only exit to the stable region is the CST.

The presence of the metastable and labile regions determines the existence of two separation mechanisms in the one-phase system: nucleophilic (between the binodal and the spinodal curves) and spinodal (inside the spinodal region). During nucleation, the separation of the metastable phase is caused by the formation of concentration fluctuations if their compositions are close to the compositions of the coexisting equilibrium phases and the size exceeds the critical value. The critical nucleus size decreases while the depth of entry into the metastable region increases. At the subsequent stages the nuclei grow from the non-equilibrium matrix solution due to the diffusion of its components. The nuclei with dimensions less than a certain critical size will defuse. At all decomposition stages, the system has two phases with a well-defined interface.

During spinodal decomposition the new phases appear as a result of fluctuations, which do not necessarily reach the critical value. In this case, the linear sizes of fluctuations do not increase; however, their amplitude, i.e. the concentration deviation from the initial value, grows. As in the case of nucleation, the separation finishes with the formation of two equilibrium phases. However, the rapid cooling preserves the non-equilibrium heterogeneous structure that is continuous throughout the entire volume of the system. Works [26-45] are dedicated to the investigation of the phase separation mechanisms.

The amorphous and crystalline phase separations are observed under different thermodynamic conditions. In amorphous polymer solutions, demixing occurs at the negative values of the second virial coefficient ( $A_2 < 0$ ); in other words, the system separation is caused by poor interaction between the polymer and the solvent. In the solutions of crystallizing polymers the phase separation takes place when  $A_2 \geq 0$ . At the approach to the liquidus curve, the value of  $A_2$  decreases as a result of the deterioration of thermodynamic affinity between the polymer and the solvent but remains positive until the system separation.

## 1.1 Types of Diagrams of Polymer–Solvent Systems

Figures 1.3–1.9 show the experimental boundary curves for some polymer–solvent systems with liquid-liquid and liquid-solid phase separation. For polymer solutions the binodals are always highly asymmetric and the critical concentrations are small as a result of the large differences in the molecular weights of the components.

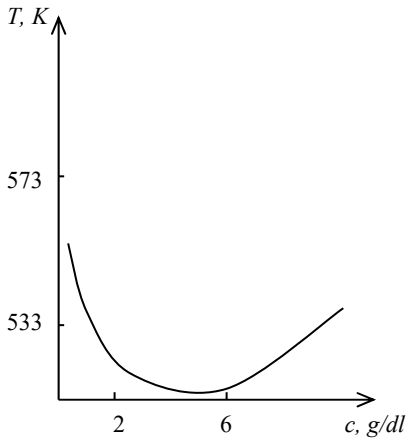


**Fig. 1.3.** Phase diagram of the polystyrene ( $M_w=3.3 \cdot 10^6$ ) – benzene system [46]

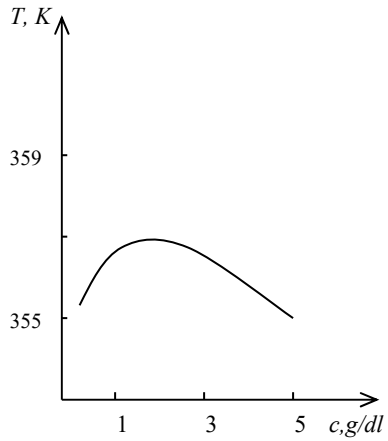


**Fig. 1.4.** Phase diagram of the PMMA ( $M_w=9.9 \cdot 10^4$ ) – butanol system [47]

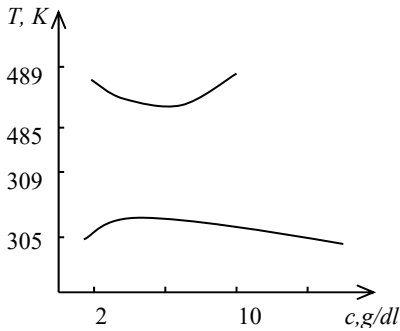


**Fig. 1.5.** Phase diagram of the polystyrene ( $M_w=3.3 \cdot 10^6$ ) – cyclohexane system [48]

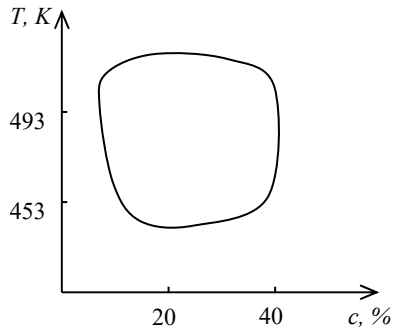


**Fig. 1.6.** Phase diagram of the polyethylene oxide – water system [49]

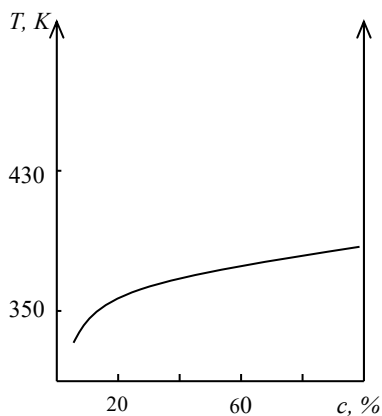


**Fig. 1.7.** Phase diagram of the polyethylene ( $M_w=2.3 \cdot 10^5$ ) – p-xylene system [50]

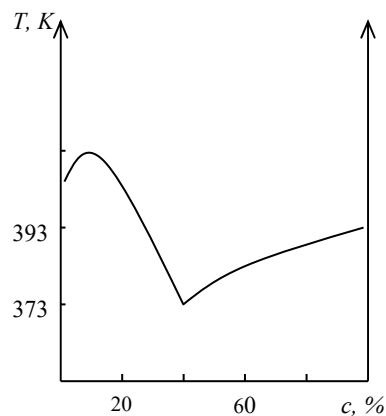


**Fig. 1.8.** Phase diagram of the polyethylene – amyl- acetate system [51]



**Fig. 1.9.** Phase diagram of the isotactic polystyrene ( $M_w=4.0 \cdot 10^5$ ) – toluene system [52]

The right branch of the liquidus curve is usually determined for the solutions of crystallizing polymers (Fig.1.9). However, both branches of the boundary curve can be determined for the system consisting of a polymer with a relatively small molecular weight ( $M \sim 10^3 - 10^4$ ) and a solvent with a high melting point [53, 54].

The boundary curve is binodal only for strictly binary systems. The solutions of unfractionated polymers are multi-component systems. The influence of polydispersity on the phase equilibrium of polymer systems has been studied in detail by Schultz and Flory [55] as well as other authors [14, 56–59]. In 1949, on the basis of the Flory-Huggins theory [60, 61], Stockmayer [59] predicted that the value of critical concentration should increase with the increase in polydispersity. Works [61–63] show that in polymolecular systems, there is an inflection point on the right branch of the boundary curve, which indicates the true value of the critical concentration of quasi-binary systems. Consequently, in this case, the maximum temperature of the boundary curve (for the systems with UCST) reflects the behavior of the highest molecular weight fraction and is actually the thermal precipitation threshold. The critical point characterizing the behavior of the whole system corresponds to the lower temperatures and higher concentrations [48, 64]. As the polymer molecular weight  $M$  increases, the UCST rises and the LCST drops due to the inferior mutual solubility of the components. The dependence of the CST on  $M$  is described by the following equation [65]:

$$1/\text{CST} = 1/\theta + K/M^{1/2},$$

where  $\theta$  is the critical temperature of dissolution of a polymer with an infinitely large molecular weight,  $M$  and  $K$  are constants for a given polymer–solvent system. At  $\theta$ -temperature (under  $\theta$ -conditions), the second virial coefficient is equal to  $A_2 = 0$ , the Flory-Huggins interaction parameter is  $\chi = 1/2$ , and the change of the chemical potential of a solvent in a solution is  $\Delta\mu_i = 0$ . In contrast to the low molecular weight liquid mixtures, while analyzing the phase behavior of solutions containing macromolecular compounds, the possibility of coil-globule transition of macromolecules needs to be considered: a collapse of the polymer chains in solution due to solvent quality deterioration. The possibility of a sharp decrease in the size of the polymer macromolecules in diluted solutions at temperatures below  $\theta$ -temperature was first mentioned in work [66].

More theoretical [67–77] and experimental [78–88] works examined this issue later. Fig. 1.10 shows the phase diagram of the polystyrene–cyclohexane system [88], which was constructed using such methods as light scattering, cloud point technique, scanning calorimetry, and using data about the volume-ratios and concentrations of the coexistent phases.

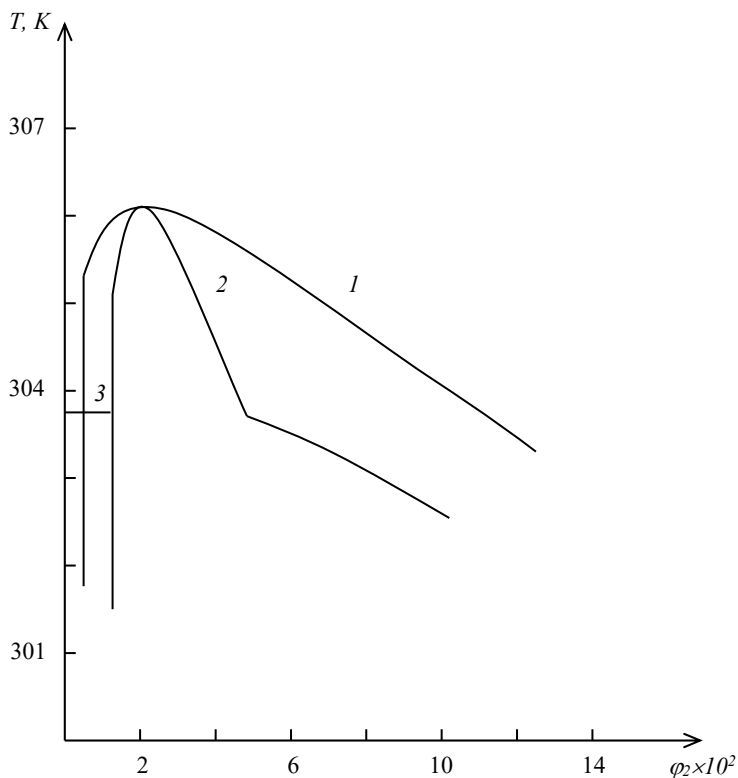


**Fig. 1.10.** Phase diagram of the PS ( $M_w=3.3 \cdot 10^6$ )–cyclohexane system: the binodal curve (1) is determined by the cloud point technique and from the data about the volume-ratios and concentrations of the coexistent phases; the spinodal curve (2) is determined by the light scattering method; the boundary curve (3) is determined by the DSC

The polymer chain collapse at one and the same temperature regardless of the solution concentration is observed in the system at 303.86 K and concentrations within  $0 < \varphi_2 < 5.5 \times 10^{-3}$ . At the same temperature there is an inflection point on the spinodal in the region of moderately concentrated solutions. Thus, the coil-globule transition is observed both in stable and metastable regions. This may be explained by their thermodynamic indistinguishability: For both regions, the second derivative of the Gibbs free energy of mixing with respect to composition is positive.



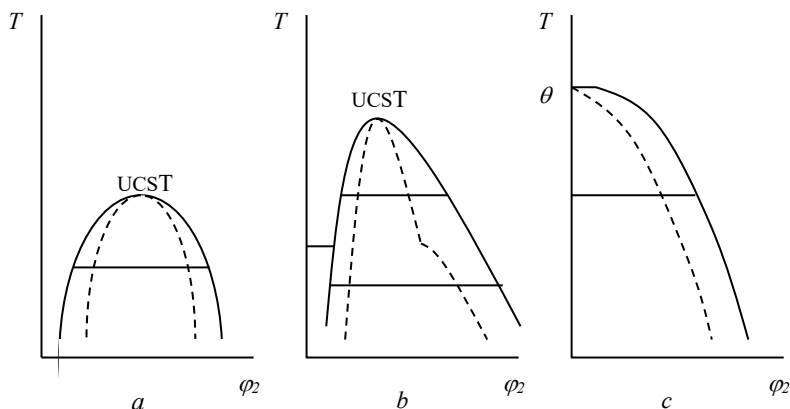


**Fig. 1.11.** Phase diagrams of the polymer–solvent systems: (a)  $M = 10^3\text{--}10^4$ , (b)  $M = 10^6\text{--}10^7$ , (c)  $M \rightarrow \infty$  (see explanations in the text)

Since the collapse of chains is impossible for macromolecules with a relatively small ( $10^3\text{--}10^4$ ) and infinitely large molecular weight  $M$ , the phase diagrams of these systems are different (Fig. 1.11, a). For solutions of the polymer with  $M \sim 10^3\text{--}10^4$  (see Fig. 1.11, a), the node connects the points corresponding to the compositions of the coexistent phases. At temperatures above the chain collapse, for the solutions of the polymer with  $M: 10^6\text{--}10^7$ , the node connects the points, one of which corresponds to the diluted solution of macromolecules in the coil conformation and the other to the concentrated solution. At temperatures below the chain collapse level, the node connects the points that correspond to the diluted solution of globules and the concentrated polymer solution (Fig. 1.11, b). For the solutions of the polymers with an infinitely large molecular weight  $M$  (Fig. 1.11, c), the critical concentration tends to zero and the node joins the points that correspond to the pure solvent and the concentrated polymer solution.

In 1956, Flory [89] proposed a theoretical diagram for a rigid-chain polymer–solvent system, which was constructed in the coordinates  $\chi - \varphi_2$  (where  $\varphi_2$  is the polymer volume fraction) (Fig. 1.12). According to this diagram, starting from a certain concentration, the polymer solutions exist in a liquid crystalline (mesomorphic) phase. Such phases were discovered for the following systems: poly- $\gamma$ -benzyl-L-glutamate

(PBG)–dimethylformamide/methanol [90], poly-p-benzamide–dimethylacetamide–LiCl [91], PBG–dioxane [92]. The phase diagrams of polymer solutions with liquid crystalline phase separation are described in the works [93, 94].

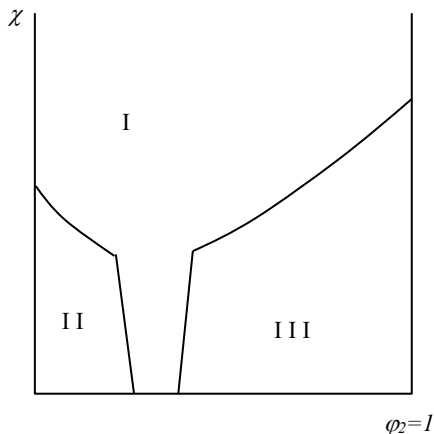


**Fig. 1.12.** Theoretical phase diagram of a rigid-chain polymer–solvent system: (I) the region of phase separation into the isotropic and anisotropic phase, (II) the region of isotropic solutions, (III) the region of anisotropic solutions [89]

Authors [95, 96] discovered a new type of boundary curve for solutions of crystallizing polymers. A characteristic feature of this curve is a horizontal segment, showing that  $T_{ph}$  does not depend on the solution concentration (Fig. 1.13). It is typical for the crystallizing polymer–solvent systems in which the polymers are of the same nature but amorphous that amorphous (liquid–liquid) demixing is realized at the critical concentration of the solution components within the range of 2–5 g/dL. The smallest thermodynamic interaction between the polymer and the solvent is observed in this concentration range. For solutions of crystallizing polymers, the following equation is true [97]:

$$\frac{1}{T_m} - \frac{1}{T_m^0} = \frac{RV_{unit}}{V_1\Delta H_{unit}} \left[ (1 - \varphi_2) - \chi(1 - \varphi_2)^2 \right],$$

where  $T_m^0$  and  $T_m$  are the melting points of the individual polymer and the polymer in contact with the solvent, respectively;  $R$  is the gas constant;

$V_{unit}$  and  $V_1$  are molar volumes of monomeric units and the solvent, respectively;  $\Delta H_{unit}$  is the molar heat of melting;  $\chi$  is the Flory-Huggins parameter;  $\varphi_2$  is the polymer volume fraction.

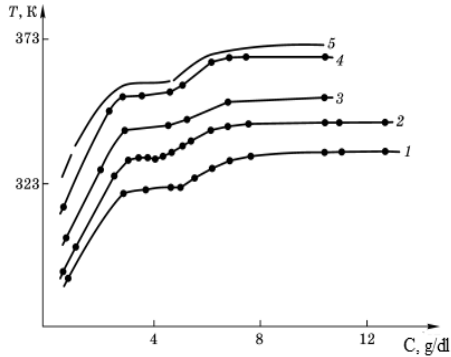


**Fig. 1.13.** Boundary curves for the isotactic PS ( $M=3.0 \cdot 10^5$ )–cyclohexane system. The solution cooling rate is 96 (1), 57 (2), 5 (3), 1 K/h (4). Curve 5 corresponds to infinitely slow cooling.

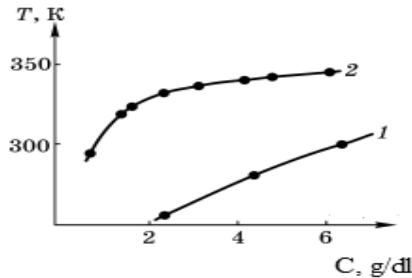


**Fig. 1.14.** Boundary curves for the isotactic PS ( $M=3.0 \cdot 10^5$ )–toluene system. Cooling rate is 1 K/h (2) and 58 K/h (1).

It follows from this equation that if the quality of the solvent is better (the Flory-Huggins parameter  $\chi$  is smaller), the melting point of polymer decreases further. For the systems with liquid-liquid demixing, a sharp deterioration of thermodynamic affinity between the polymer and the solvent is observed in moderately concentrated solutions. Consequently, within this composition range, the temperature  $T_{ph}$  will change insignificantly in case of the crystalline phase separation. For the solutions of the same polymers in good solvents, in which amorphous phase

separation is impossible, the boundary curve has the form of a typical liquidus curve (Fig. 1.14).

In the solutions of stereoregular polymers, which can form macromolecular stereocomplexes (Fig. 1.15, 1.16) [98], the boundary curves take unusual shapes, showing the constant temperatures  $T_{ph}$  within a wide range of compositions (up to 50% of the polymer). The stereocomplexes play the role of the physical knots in the forming spatial network. When the temperature decreases, the number of knots increases, which results in the phase separation of the solution and subsequent gelation.

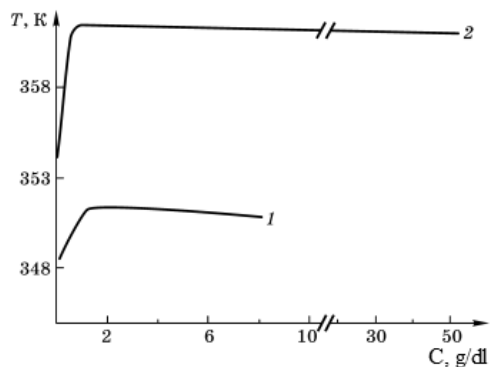


**Fig. 1.15.** Boundary curves of the PMMA–butanol system (1), and PMMA–hexanol system (2).

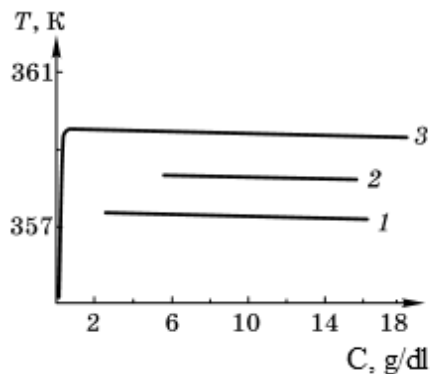


**Fig. 1.16.** Boundary curves of the PMMA–hexanol system, at cooling rates 230 (1), 91 (2) and 2 K/h (3).

## 1.2 Effect of Size and Shape of Solvent Molecules on Phase Transitions in Polymer Solutions

Many theoretical studies of polymer solutions have been dedicated to the dependence between the polymer molecular weight  $M$ , i.e. the macromolecular sizes, and the critical solution temperatures. Flory's equation also connects the critical solution temperature with the polymer molecular weight  $M$ . Theoretically, the interaction between the polymer and the solvent should become worse with the growth of  $M$ . This is manifested in the displacement of the bimodal curve, decrease of the LCST, increase of the UCST and in the corresponding changes in the  $\theta$ -temperatures. However, it is experimentally shown that the size and the spatial shape of the solvent molecules also have a significant effect on these parameters. For example, in the case of PP solutions ( $M = 2.42 \times 10^5$ ), it was found [99] that in alkanes, when n-pentane was substituted by n-nonane, the LCST increased from 422 to 571 K, meaning an increase by  $\sim 37$  K per  $\text{CH}_2$  group; and when n-pentane was replaced by cyclopentane or n-hexane was replaced by cyclohexane, the LCST increased by 73 and 70 K, respectively. A similar phenomenon was observed [99] in the PE solutions ( $M = 1.34 \times 10^5$ ): When n-pentane was substituted by n-nonane, the LCST increased from 353 to 531 K, meaning an increase by  $\sim 44$  K per  $\text{CH}_2$ ; and when n-pentane was replaced by cyclopentane or n-hexane by cyclohexane, the LCST increased by 119 and 107 K, respectively. For the polybutene-1 solutions ( $M = 5.3 \times 10^5$ ), it was proved [100] that in alkanes, in the case of replacement of n-pentane by n-nonane, the LCST increases from 421 to 564 K, meaning an increase by  $\sim 36$  K per  $\text{CH}_2$  group while for the polypentene-1 solutions ( $M = 4.65 \times 10^6$ ) it was equal to 41 K. A similar phenomenon was observed for the PS solutions in alkyl acetates [101]: after the substitution of methyl acetate to decyl acetate, the lower  $\theta_L$ -temperature rose from 409 K to 643 K. For the PP solution in pentane, hexane and heptane  $\theta_L = 397$  K, 441 K and 483 K, respectively, that meant an increase by  $\sim 43$  K per  $\text{CH}_2$  group. The  $\theta_L$ -temperatures of the PMMA solutions in acetone, methyl ethyl ketone and diethyl ketone were 439, 482 and 506 K, respectively, meaning an average increase by 39 K per  $\text{CH}_2$  group [102]. For the PIB and PDMS solutions in alkanes, in the series from pentane to dodecane, the  $\theta_L$ -temperatures increased from 346 to 585 K (PIB) and from 453 to 643 K (PDMS), respectively [103]. A similar phenomenon was observed for the PIB solutions in alkanes and described in works [104, 105]. It was shown in [106] that for the PS solutions ( $M = 3.3 \times 10^6$ ) in benzene, the LCST is 56 K lower than in

ethylbenzene. A similar  $\theta_L$ -temperature dependence was also found in these systems [107].

The change in the solvent molecular size and shape influences phase transitions under cooling, which is typical for the systems with UCST. It was shown [108] that if in the solutions of poly-*n*-butyl methacrylate in alkanes *n*-octane is substituted by *n*-hexadecane, the  $\theta_U$ -temperature rises from 342.1 to 393 K, meaning an increase of  $\sim 6$  K per  $\text{CH}_2$  group. For the solutions of poly-2-methyl-5-vinylpyridine in propyl acetate, butyl acetate, amyl acetate, the  $\theta_U$ -temperature increases from 292.5 to 321.4 K [109]. It was shown [110] that when poly(ethyl-acrylate) is dissolved in alcohols in the series from methanol to *n*-butanol, the  $\theta_U$ -temperature increases from 293.7 to 318.1 K, which means if a  $\text{CH}_2$  group is added to the alkyl radical, the  $\theta_U$ -temperature grows by 8 K. A similar phenomenon is reported in work [111] for the PS solutions in cyclohexane ( $\theta_U = 307$  K) and ethyl-cyclohexane ( $\theta_U = 343$  K).

The growth of the solvent molecules can result in the decrease of UCST. It was shown in [112]  $\theta_U$ -temperatures of 268, 245, and 217 K for the PDMS solution in benzene, toluene, and xylene, respectively. A similar dependence has been discovered for the PIB solutions in the same solvents [112].

More detailed information about the phase diagrams of polymer solutions in the homologous series of solvents can be found in works [113, 114]. The review of this experimental data shows that the increase of the solvent molecular size causes a significant increase of the LCST and a less essential increase or decrease of the UCST. The authors of the cited papers changed the size of the macromolecules or the solvent molecules.

Work [115] is dedicated to the research of the phase transitions in the systems in which the size of the molecules of the two components was consistently changed. The author studied the solutions of polypropylene glycols (PPG) with  $M_w = 1100$  ( $M_w/M_n = 1.10$ ) PPG-1; 2000 ( $M_w/M_n = 1.15$ ) PPG-2; 3100 ( $M_w/M_n = 1.05$ ) PPG-3; and 6900 ( $M_w/M_n = 1.05$ ) PPG-4 in *n*-hexane, *n*-octane, *n*-decane, *n*-dodecane, *n*-tetradecane, and *n*-hexadecane.

Figure 1.17 shows boundary curves for the PPG solutions in *n*-hexane. It is quite evident that upon cooling, these systems demix, i.e. they have UCST. As the polymer molecular weight  $M$  increases, the critical point is displaced to the region of the lower PPG concentrations. The thermodynamic criteria of UCST are the positive values of the enthalpy and entropy of mixing [116]. Indeed, the authors [117] proved that PPG was dissolved in hexane with the absorption of heat and increase of entropy. In addition, the cohesive energy between similar molecules is